

Estimating the velocity profile and acoustical quantities of a harmonically vibrating membrane from on-axis pressure data

Ronald M. Aarts^{1,2}, A.J.E.M.Janssen³

¹ Philips Research, HTC 36, 5656AE Eindhoven, The Netherlands

² Technical University Eindhoven, PT3.23, P.O Box 513, 5600MB Eindhoven, The Netherlands

Email ¹: Ronald.M.Aarts@philips.com, Email ³: A.J.E.M.Janssen@philips.com

Introduction

In this paper an analytic method developed in [1, 2] for the calculation of acoustical quantities such as the sound pressure on-axis, far-field, directivity, and the total radiated power is presented. This method is based on the analytical results as developed in the diffraction theory of optical aberrations by Nijboer [3] and Zernike and Nijboer [4], see also [5, 6]. Using this approach, many of the analytic results in Greenspan [7], such as those on the sound pressure on-axis, the total radiated power, and the results in text books [8] on far-field expressions and directivity can be presented and extended in a systematic fashion. This is worked out in [1] for the results on on-axis pressure and far-field expressions for arbitrary velocity distributions on flat piston radiators. The mathematical foundation of these methods related to directivity and the total radiated power is discussed in [2]. An arbitrary velocity distribution can be efficiently developed as a series in Zernike polynomials. Using near-field pressure measurements on-axis the coefficients of these polynomials can be estimated. With these estimated coefficients the acoustical quantities mentioned above can be estimated as well. An immediate application is to predict the far-field sound pressure from near-field pressure data measured without using an anechoic chamber (generalized Keele scheme [1, 9]).

The radiated pressure is given in integral form by the Rayleigh integral [8, 10] as

$$p(\underline{r}, t) = \frac{i\rho_0 ck}{2\pi} e^{i\omega t} \int_S v(\underline{r}_s) \frac{e^{-ikr'}}{r'} dS, \quad (1)$$

where ρ_0 is the density of the medium, c is the speed of sound in the medium, $k = \omega/c$ is the wave number and ω is the radian frequency of the harmonically vibrating surface S . Furthermore, t is time, \underline{r} is a field point, \underline{r}_s is a point on the surface S , $r' = |\underline{r} - \underline{r}_s|$ is the distance between \underline{r} and \underline{r}_s , and $v(\underline{r}_s)$ is the normal component of a (not necessarily uniform) velocity profile on the surface S . The time variable t in $p(\underline{r}, t)$ and the harmonic factor $\exp(i\omega t)$ in front of the integral in Eq. (1) will be omitted in the sequel. For transparency of exposition, the surface S is assumed [1, 2] to be a disk of radius a , $|\underline{r}_s| = r_s \leq a$, with average velocity V_s given by

$$V = \int_S v(\underline{r}_s) dS = V_s \pi a^2. \quad (2)$$

In [1] a generalization to the case of dome-shaped

radiator surfaces S is done. See Fig. 1 for the geometry and notations used in the case of a flat piston.

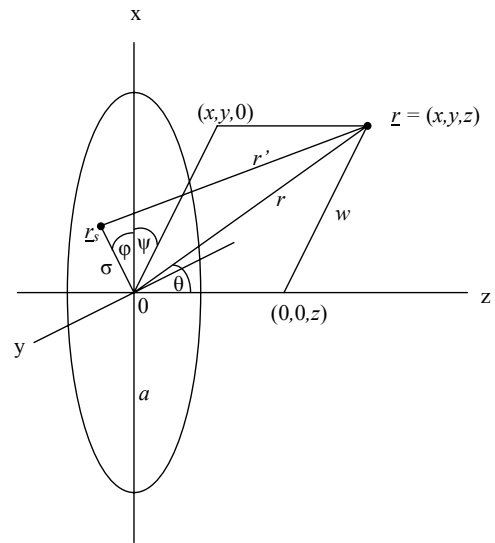


Figure 1: Set-up and notations.

$$\begin{aligned} \underline{r}_s &= (x_s, y_s, 0) = (\sigma \cos \varphi, \sigma \sin \varphi, 0) \\ \underline{r} &= (x, y, z) = (r \sin \theta \cos \psi, r \sin \theta \sin \psi, r \cos \theta) \\ w &= r \sin \theta = (x^2 + y^2)^{1/2}, \quad z = r \cos \theta \\ r &= |\underline{r}| = (x^2 + y^2 + z^2)^{1/2} = (w^2 + z^2)^{1/2} \\ r' &= |\underline{r} - \underline{r}_s| = (r^2 + \sigma^2 - 2\sigma w \cos(\psi - \varphi))^{1/2}. \end{aligned}$$

Frankort [11] has shown that loudspeaker cones mainly vibrate in a radially symmetric fashion. Therefore the attention in this paper is restricted to radially symmetric velocity distributions v , which are denoted as $v(\sigma)$, $0 \leq \sigma \leq a$. Under an integrability condition, these v 's admit a representation

$$v(\sigma) = V_s \sum_{n=0}^{\infty} u_n R_{2n}^0(\sigma/a), \quad 0 \leq \sigma \leq a, \quad (3)$$

in which the u_n are scalar coefficients and

$$R_{2n}^0(\rho) = P_n(2\rho^2 - 1), \quad 0 \leq \rho \leq 1, \quad (4)$$

where P_n are the Legendre polynomials [12]. In [1] there are presented analytical results for the on-axis and far-field pressure $p(\underline{x})$ in Eq. (1) related to the coefficients u_n and polynomials R_{2n}^0 occurring in the expansion in Eq. (3). By orthogonality of the terms $R_{2n}^0(\rho)$, the coefficients u_n in Eq. (3) can be found in integral form

as

$$u_n = \frac{2(2n+1)}{V_s} \int_0^1 R_{2n}^0(\rho) v(a\rho) \rho d\rho, \quad n = 0, 1, \dots \quad (5)$$

In particular, $u_0 = 1$. There is an impressive number of cases where one can explicitly find the u_n in Eq. (5); these include the rigid piston ($\ell = 0$), the simply supported radiator ($\ell = 1$) and the higher order clamped radiators ($\ell \geq 2$) with the velocity profile given by

$$v^{(\ell)}(\sigma) = (\ell + 1) V_s (1 - (\sigma/a)^2)^\ell H(a - \sigma), \quad \ell = 0, 1, \dots, \quad (6)$$

and the Gaussian velocity profile

$$v(\sigma; \alpha) = \frac{\alpha V_s}{1 - e^{-\alpha}} e^{-\alpha(\sigma/a)^2} H(a - \sigma), \quad (7)$$

where $H(x)$ is the Heaviside function, $H(x) = 0, 1/2$, or 1 according as x is negative, zero, or positive. Hence, the velocity profiles in Eqs. (6) and (7) vanish for $\sigma > a$.

The Zernike terms R_{2n}^0

The Zernike terms R_{2n}^0 are polynomials of degree $2n$ given by

$$R_{2n}^0(\sigma/a) = P_n(2(\sigma/a)^2 - 1) = \sum_{s=0}^n (-1)^s \binom{2n-s}{n} \binom{n}{s} (\sigma/a)^{2n-2s}, \quad (8)$$

where P_n is the Legendre polynomial of degree n , see Ref. [12, 22.3.8 and 22.5.42]. The first few R_{2n}^0 are given in Table 1. In [1][Appendix A], a number of cases are listed, such as the expansion

$$(1 - (\sigma/a)^2)^\ell = \sum_{n=0}^{\ell} (-1)^n \frac{2n+1}{n+1} \frac{\binom{\ell}{n}}{\binom{\ell+n+1}{\ell}} R_{2n}^0(\sigma/a), \quad (9)$$

which are relevant for the rigid and simply supported ($\ell = 0, 1$) and the clamped radiators ($\ell \geq 2$).

Table 1: Zernike polynomials

n	$R_{2n}^0(\sigma/a)$
0	1
1	$2(\sigma/a)^2 - 1$
2	$6(\sigma/a)^4 - 6(\sigma/a)^2 + 1$
3	$20(\sigma/a)^6 - 30(\sigma/a)^4 + 12(\sigma/a)^2 - 1$

On-axis and far-field expressions

The velocity profile $v(\sigma)$ considered in this section (normal component) vanishes outside the disk $\sigma \leq a$ and has been developed into a Zernike series as in Eq. (3) with coefficients u_n given in accordance with Eq. (5) or explicitly as in the case given in Eq. (9).

On-axis expression

There holds [1] for an on-axis point $\underline{r} = (0, 0, r)$ with $r \geq 0$ the formula

$$p(\underline{r}) = \frac{1}{2} \rho_0 c V_s (ka)^2 \sum_{n=0}^{\infty} \gamma_n(k, r) u_n, \quad (10)$$

in which

$$\gamma_n(k, r) = (-1)^n j_n(kr_-) h_n^{(2)}(kr_+), \quad (11)$$

$$r_{\pm} = \frac{1}{2} (\sqrt{r^2 + a^2} \pm r).$$

The r_{\pm} in Eq. (11) satisfy

$$0 \leq r_- \leq \frac{1}{2} a \leq r_+, \quad r_+ r_- = \frac{1}{4} a^2, \quad r_+ + r_- = \sqrt{r^2 + a^2}. \quad (12)$$

The j_n and $h_n^{(2)} = j_n - i y_n$ are the spherical Bessel and Hankel function, respectively, of the order $n = 0, 1, \dots$, see Ref. [12, § 10.1.]. In particular, $j_0(z) = (\sin z)/z$ and $h_0^{(2)}(z) = (i e^{-iz})/z$.

The result in Eqs. (10) and (11) comprises the known result [8, 8.31a,b] for the rigid piston ($\ell = 0$ in Eq. (9) and $u_0 = 1, u_1 = u_2 = \dots = 0$) with $p(\underline{r}), \underline{r} = (0, 0, r)$, given by

$$p(\underline{r}) = \frac{1}{2} \rho_0 c V_s (ka)^2 \frac{\sin kr_-}{kr_-} \frac{i e^{-ikr_+}}{kr_+} = 2i \rho_0 c V_s e^{-\frac{1}{2} ik((r^2 + a^2)^{\frac{1}{2}} + r)} \sin \frac{1}{2} k((r^2 + a^2)^{\frac{1}{2}} - r), \quad (13)$$

and it generalizes immediately to the case of the simply supported radiator ($\ell = 1$) and the clamped radiators ($\ell \geq 2$) through Eq. (9).

Far-field expression

Using the Zernike expansion Eq. (3) of $v(\sigma)$ it is shown in [1][Appendix B] that the following far-field approximation holds: when $\underline{r} = (r \sin \theta, 0, r \cos \theta)$ and $r \rightarrow \infty$,

$$p(\underline{r}) \approx i \rho_0 c k V_s \frac{e^{-ikr}}{r} a^2 \sum_{n=0}^{\infty} u_n (-1)^n \frac{J_{2n+1}(ka \sin \theta)}{ka \sin \theta}. \quad (14)$$

Some comments on the behavior of the terms $J_{2n+1}(z)/z$, $z = ka \sin \theta$, as they occur in the series in Eq. (14) are presented now. From the asymptotics of the Bessel functions, as given in Ref. [12, Eq. 9.3.1], it is seen that in the series in Eq. (14) only those terms contribute significantly for which $2n+1 \leq \frac{1}{2} e ka \sin \theta$. In particular, when $\theta = 0$, it is only the term with $n = 0$ that is non-vanishing, and this yields

$$p((0, 0, r)) \approx \frac{1}{2} i \rho_0 c V_s k a^2 \frac{e^{-ikr}}{r}, \quad r \rightarrow \infty. \quad (15)$$

This is in agreement with what is found from Eq. (10) when only the term with $n = 0$ is retained and r_+ is replaced by r , r_- is replaced by 0 . For small values of ka the terms in the series Eq. (14) decay very rapidly with n . For large values of ka , however, a significant number of terms may contribute, especially for angles θ far from 0 .

Power output and directivity

The power is defined as the intensity pv^* integrated over the plane $z = 0$. Thus, because v vanishes outside S ,

$$P = \int_S p(\sigma)v^*(\sigma)dS, \quad (16)$$

where $p(\sigma) = p((\sigma \cos \psi, \sigma \sin \psi, 0))$ is the pressure at an arbitrary point on S .

In [2] it is shown that

$$P = 2\pi i \rho_0 c k \int_0^\infty \frac{V(u)V^*(u)}{(u^2 - k^2)^{1/2}} u du, \quad (17)$$

where

$$V(u) = \int_0^a J_0(u\sigma) v(\sigma) \sigma d\sigma, \quad u \geq 0, \quad (18)$$

is the Hankel transform (of order 0) of v , see [2][Sec.V.B], for more details.

We next consider the directivity. With the usual approximation arguments in the Rayleigh integral representation of p in Eq. (1), there follows ($\underline{r} = (r \cos \psi \sin \theta, r \sin \psi \sin \theta, r \cos \theta)$)

$$p(\underline{r}) \approx i \rho_0 c k \frac{e^{-ikr}}{r} V(k \sin \theta). \quad (19)$$

From this there results the directivity

$$D = \frac{4\pi |V(0)|^2}{\int_0^{2\pi} \int_0^{\pi/2} |V(k \sin \theta)|^2 \sin \theta d\psi d\theta} \\ = \frac{2|V(0)|^2}{\int_0^{\pi/2} |V(k \sin \theta)|^2 \sin \theta d\theta}, \quad (20)$$

see Kinsler et al. [8], Sec.8.9. By Eqs. (2) and (18) it holds that $V(0) = \frac{1}{2}a^2 V_s$. Next consider the case that $ka \rightarrow \infty$. It is shown in [2][Sec. V.D] that

$$D \approx \frac{2(\frac{1}{2}a^2 V_s)^2}{\frac{1}{2\pi \rho_0 c k^2} 2\pi \rho_0 c a^2 \int_0^1 |v(a\rho)|^2 \rho d\rho} \\ = \frac{\frac{1}{2}(ka)^2 V_s^2}{\int_0^1 |v(a\rho)|^2 \rho d\rho} = C_v (ka)^2, \quad (21)$$

in which C_v is the ratio of the square of the modulus of the average velocity and the average of the square of the modulus of the velocity (averages over S). In case that $v = v^{(\ell)}$, the last member of Eq. (21) is given by $(2\ell + 1)(\ell + 1)^{-1}(ka)^2$; in Kinsler et al. [8], end of Subsec. 8.9. this result for the case $\ell = 0$ is given.

Estimating velocity profiles from on-axis radiation

The on-axis expression Eqs. (10)–(11) for the pressure can, in reverse direction, be used [1] to estimate the velocity profile on the disk from (measured) on-axis data via its expansion coefficients u_n . This can be effectuated by adopting a matching approach in which the coefficients u_n in the ‘theoretical’ expression Eqs. (10)–(11) are determined so as to optimize the match with

measured data at $M + 1$ points. Thus, one has for the pressure $p_m = p((0, 0, r_m))$ due to the velocity profile $v(\sigma) = V_s \sum_{n=0}^N u_n R_{2n}^0(\sigma/a)$ the expression

$$p_m = \frac{1}{2} \rho_0 c V_s (ka)^2 \sum_{n=0}^N (-1)^n j_n(kr_{m,-}) h_n^{(2)}(kr_{m,+}) u_n, \quad (22)$$

where $r_m \geq 0$ and

$$r_{m,\pm} = \frac{1}{2}(\sqrt{r_m^2 + a^2} \pm r_m), \quad (23)$$

and $m = 0, 1, \dots, M$. With

$$A = (A_{mn})_{\substack{m=0,1,\dots,M, \\ n=0,1,\dots,N}}, \quad (24)$$

$$A_{mn} = \frac{1}{2} \rho_0 c V_s (ka)^2 j_n(kr_{m,-}) h_n^{(2)}(kr_{m,+}),$$

$$\underline{p} = [p_0, \dots, p_M]^T, \quad \underline{u} = [u_0, \dots, u_N]^T, \quad (25)$$

the relation between on-axis pressures p_m and coefficients u_n can be concisely written as

$$A \underline{u} = \underline{p}. \quad (26)$$

Now given a (noisy) on-axis data vector \underline{p} , one can estimate the coefficients vector \underline{u} by adopting a least mean-squares approach for the error $A \underline{u} - \underline{p}$. This will be illustrated by an experiment, below.

For the experiment, we measured a loudspeaker (vifa MG10SD09-08, $a = 3.2$ cm) in an IEC-baffle [13], at 10 near-field positions ($r_m = 0.00, 0.01, 0.02, 0.03, 0.04, 0.05, 0.07, 0.10, 0.13, 0.19$ m), and, finally, for the far-field at 1 m distance. For a particular frequency at 13.72 kHz ($ka = 8.0423$), the magnitude of the sound pressure is plotted in Fig. 2 (solid curve ‘ p meas’). Using the same procedure as described above for the first simulation, the inverse process was followed by using the ten measured near-field pressure data points to estimate the coefficients vector \underline{u} . Using four Zernike coefficients the pressure data were recovered and plotted in Fig. 2 (dotted curve ‘ p rec’). It appears that the two curves show good resemblance to each other and that only four coefficients are needed to provide a very good description of the near-field at rather high frequencies (13.72 kHz). Furthermore, it appears that using these four coefficients, the calculated sound pressure level at 1-m distance yields -42 dB. The measured value at that far-field point is -44 dB. These values match rather closely, even though the cone vibrates not fully circularly symmetric anymore at the used frequency of 13.72 kHz, due to break-up behavior. This match provides a proof of principle as the far-field measurement point was not used to determine the Zernike coefficients.

In the experiment just described, no particular effort was spent in forming and handling the linear systems so as to have small condition numbers. The condition number, the ratio of the largest and smallest non-zero singular value of the matrix A in Eq. (24), equals 50 in the case of the loudspeaker experiment leading to Fig. 2. In practical cases the number of required Zernike coefficients will be less than, say, six. This will not cause numerical difficulties. Furthermore, such a modest number of coefficients already parameterizes a large set of velocity profiles.

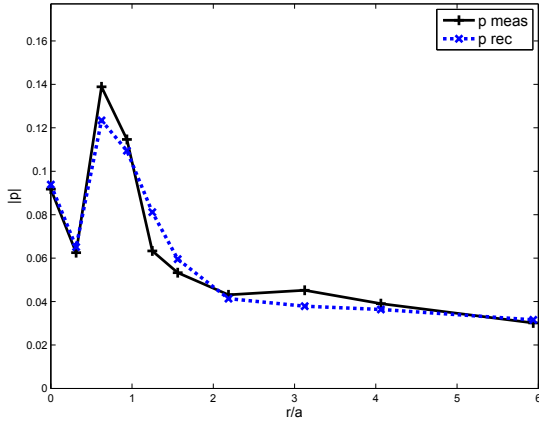


Figure 2: Measured loudspeaker at 13.72 kHz ($ka = 8.0423$, p meas, solid curve) vs. r/a . Recovered pressure data (p rec dotted curve).

Far-field assessment from on-axis measurements

In Keele [9] a method is described to assess low-frequency loudspeaker performance in the on-axis far-field from an on-axis near-field measurement. In the case of the rigid piston, the on-axis pressure $p(r) = p((0, 0, r))$ is given by Eq. (13). Now assume $ka \ll 1$. When $r \ll a$ it holds that

$$\sin\left(\frac{1}{2}k\sqrt{r^2 + a^2} - r\right) \approx \sin\left(\frac{1}{2}ka\right) \approx \frac{1}{2}ka, \quad (27)$$

and, when $r \gg a$ it holds that

$$\sin\left(\frac{1}{2}k\sqrt{r^2 + a^2} - r\right) \approx \sin\left(\frac{ka^2}{4r}\right) \approx \frac{ka^2}{4r}. \quad (28)$$

Therefore, the ratio of the moduli of near-field and far-field on-axis pressure is given by $2r/a$. This is the basis of Keele's method; it allows far-field loudspeaker assessment without having to use an anechoic room.

With the inversion procedure to estimate velocity profiles from on-axis data (which are taken in the relative near-field) and with the forward calculation scheme for the far-field as described above it is now possible to generalize Keele's scheme.

Conclusions

Zernike polynomials are an efficient and robust method to describe velocity profiles of resilient sound radiators. A wide variety of velocity profiles, including the rigid piston, the simply supported radiator, the clamped radiators, Gaussian radiators as well as real loudspeaker drivers, can be approximated accurately using only a few terms of their Zernike expansions. This method enables one to solve both the forward as well as the inverse problem. With the forward method the on-axis and far-field off-axis sound pressure are calculated for a given velocity profile. With the inverse method the actual velocity profile of the radiator is estimated using (measured) on-axis sound pressure data. This computed velocity profile allows the extrapolation to

far-field loudspeaker pressure data, including off-axis behavior, without the use of anechoic rooms.

References

- [1] R.M. Aarts and A.J.E.M. Janssen. On-axis and far-field sound radiation from resilient flat and dome-shaped radiators. *J. Acoust. Soc. Am.*, 125(3), March 2009.
- [2] R.M. Aarts and A.J.E.M. Janssen. Sound radiation quantities arising from a resilient circular radiator. Submitted to *J. Acoust. Soc. Am.*, 31 Oct. 2008.
- [3] B.R.A. Nijboer. *The diffraction theory of aberrations*. Ph.D. dissertation, University of Groningen, The Netherlands, 1942.
- [4] F. Zernike and B.R.A. Nijboer. The theory of optical images (published in French as La théorie des images optiques). *Revue d'Optique*, Paris, pp. 227-235, 1949.
- [5] M. Born and E. Wolf. *Principles of Optics*, 7th ed. Cambridge University Press, Cambridge, Chap. 9, 2002.
- [6] J.J.M. Braat, S. van Haver, A.J.E.M. Janssen, and P. Dirksen. Assessment of optical systems by means of point-spread functions. In *Progress in Optics* (Vol. 51) edited by E. Wolf (Elsevier, Amsterdam), Chap. 6, 2008.
- [7] M. Greenspan. Piston radiator: Some extensions of the theory. *J. Acoust. Soc. Am.*, 65:608–621, 1979.
- [8] L.E. Kinsler, A.R. Frey, A.B. Coppens, and J.V. Sanders. *Fundamentals of Acoustics*. Wiley, New York, 1982.
- [9] D.B. (Don) Keele, Jr. Low-frequency loudspeaker assessment by nearfield sound-pressure measurement. *J. Audio Eng. Soc.*, 22(3):154–162, April 1974.
- [10] J.W.S. Rayleigh. *The Theory of Sound, Vol. 2, 1896*. (reprinted by Dover, New York), 1945.
- [11] F.J.M. Frankort. *Vibration and Sound Radiation of Loudspeaker Cones*. Ph.D. dissertation, Delft University of Technology, 1975.
- [12] M. Abramowitz and I.A. Stegun. *Handbook of Mathematical Functions*. Dover, New York, 1972.
- [13] International Electrotechnical Commission (IEC), Geneva, Switzerland. IEC 60268-5 Sound System Equipment - Part 5: Loudspeakers, 2007